Bull. Nov. Comp. Center, Num. Anal., 12 (2003), 21–28

Numerical solution of 3D equations of motion*

Y.L. Gurieva, V.P. Il'in

1. Introduction

We consider algorithms of numerical solution of a nonlinear system of three diffusion-convection partial differential equations (PDEs)

$$
\begin{aligned}
&L(\vec{u})u + \frac{\partial p}{\partial x} = f_x, \quad L(\vec{u})v + \frac{\partial p}{\partial y} = f_y, \quad L(\vec{u})w + \frac{\partial p}{\partial z} = f_z, \\
&L(\vec{u}) = L^c(\vec{u}) - \left(\frac{\partial^2}{\partial x^2} + \frac{\partial^2}{\partial y^2} + \frac{\partial^2}{\partial z^2}\right), \\
&L^c(\vec{u})s = \frac{\partial(us)}{\partial x} + \frac{\partial(vs)}{\partial y} + \frac{\partial(ws)}{\partial z},
\end{aligned}
\tag{1}
$$

which are the main part of a stationary Navier–Stokes problem (the latter is added/closed by the continuity equation $\operatorname{div}\vec{u} = 0$, $\vec{u} = (u, v, w)$). Here u, v, w are the velocity components and p is a known pressure as well as the right-hand side functions f_x, f_y, f_z.

There are many publications dealing with approximations of PDEs (1) by finite difference, finite element and finite volume methods (FDM, FEM, FVM, see [1–3], for example). We consider an exponential type FVM approach, whose idea is presented in [4, 5] for a single diffusion–convection equation. The main features of the obtained system of nonlinear algebraic equations (SNLAE) are: second order of accuracy $O(h^2)$ on the uniform grid and the absolute monotonicity in a sense that matrix A is a monotonic matrix ($A^{-1} > 0$) independent of mesh-size values and the velocity component signs, for a given velocity $\vec{u}$.

The resulted SNLAE is solved by a two-level iterative process. The external one presents the relaxed nonlinear iterations for velocities, at each step the block linear system (SLAE) for the given coefficients u, v, w is solved by a biconjugate minimum residual method with multiple restarts.

*Supported by the Russian Foundation for Basic Research under Grants 02-01-01176, 01-07-90367, and NWO–RFBR under Grant 047-008-007.

This paper is organized as follows. In Section 2, we describe the numerical methods. Sections 2 and 3 have a short description of the code and results of numerical experiments, respectively.

2. Numerical approaches

For every velocity equation, we use the FVM approximation on the parallelepipedoidal nonuniform grid

$$x_{i+1} = x_i + h_i^x, \qquad y_{j+1} = y_j + h_j^y, \qquad z_{k+1} = z_k + h_k^z,$$
$$i = 0, \ldots, I, \qquad j = 0, \ldots, J, \qquad k = 0, \ldots, K.$$

We construct the Dirichlet–Voronoi cell around each grid node with the indices i, j, k

$$V_{i,j,k} = \{x_{i-1/2} < x < x_{i+1/2},\ y_{j-1/2} < y < y_{j+1/2},\ z_{k-1/2} < z < z_{k+1/2}\}$$

and denote its surface by $S_{i,j,k}$.

The approximation of equation (1) is based on the divergent form of operator L:

$$L(\vec{u})s \equiv \frac{\partial}{\partial x}\Big(-\frac{\partial s}{\partial x} + us\Big) + \frac{\partial}{\partial y}\Big(-\frac{\partial s}{\partial y} + vs\Big) + \frac{\partial}{\partial z}\Big(-\frac{\partial s}{\partial z} + ws\Big). \qquad (2)$$

Taking the integral of anyone of equations (1) for different functions $s = u$, $s = v$, or $s = w$ over the cell $V_{i,j,k}$, we come to the balance relation

$$\int\limits_{S_{i,j,k}} J^n ds = \int\limits_{V_{i,j,k}} g_s \, dV, \qquad (3)$$

where g_s depends on one of the right-hand side functions and one of the pressure gradient components, and $\vec{u}_n$, $J^n = \frac{\partial s}{\partial n} + \vec{u}_n s$ are the velocity component and the density of the flux in the direction of the outer normal to $S_{i,j,k}$.

To construct approximations of (3) we use the approach presented in [5] thus introducing two new functions μ and ϕ to make a new representation of the flux, say, over the cell surface perpendicular to x-axis:

$$J^x = -\frac{\partial s}{\partial x} + us = -\frac{1}{\mu}\frac{\partial \mu s}{\partial x}, \quad \mu = e^{-\phi}, \quad \phi = \int\limits_0^x u \, dx'.$$

Hence follows, e.g.,

$$(\mu s)_{i,j,k} - (\mu s)_{i+1,j,k} = \int\limits_{x_i}^{x_{i+1}} \mu J^x dx = J^x_{0,3} \int\limits_{x_i}^{x_{i+1}} e^{-\phi} dx + O(h^3),$$

where h is a typical mesh size and the notation $J^x_{0,3}$ corresponds to the value of the flux at the midpoint between the nodes with local numbers 0 and 3 (figure). Then we use a linear interpolation of ϕ, take exactly the exponential integral, and reject a truncation error. We obtain the difference representation of the flux density

$$J^{x,h}_{0,3} = \frac{\phi_0 - \phi_3}{h^x_i}\Big(\frac{s_0}{exp(\phi_0 - \phi_3) - 1} - \frac{s_3}{1 - exp(\phi_3 - \phi_0)}\Big).$$

Introducing the notation $S_x = h^y_j h^z_k/4$ and using approximation

$$\phi_3 - \phi_0 = \int_{x_i}^{x_{i+1}} u\,dx \approx h^x_i \frac{u_0 + u_3}{2},$$

we approximate the left-hand side of equation (3) by a simple quadrature

$$I^{x,h}_{0,3} = S_x J^{x,h}_{0,3} = a^x_{0,0} s_0 - a^x_{0,3} s_3.$$

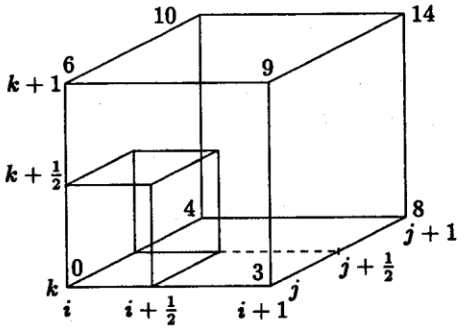

Local node numbering on a grid cell

Here we have already introduced elements of the local balance matrix

$$a^x_{0,0} = \frac{S_x u_{0,3}}{1 - c^{-1}_{0,3}} = a^x_{0,3} c_{0,3}, \qquad a^x_{0,3} = \frac{S_x u_{0,3}}{c_{0,3} - 1},$$

$$u_{0,3} = \frac{u_0 + u_3}{2}, \qquad c_{0,3} = \exp(h^x_i u_{0,3})$$

in order that the element-by-element approach be used for obtaining the global matrix. In the same way one can define the rest entries of the local balance matrix, e.g.,

$$a^y_{0,0} = a^y_{0,4} c_{0,4}, \qquad a^y_{0,4} = \frac{S_y v_{0,4}}{c_{0,4} - 1},$$

$$v_{0,4} = \frac{v_0 + v_4}{2}, \quad c_{0,4} = \exp(h^y_j v_{0,4}), \quad S_y = \frac{h^x_i h^z_k}{4},$$

$$a^z_{0,0} = a^z_{0,6} c_{0,6}, \qquad a^z_{0,6} = \frac{S_z w_{0,6}}{c_{0,6} - 1},$$

$$w_{0,6} = \frac{w_0 + w_6}{2}, \quad c_{0,6} = \exp(h^z_k w_{0,6}), \quad S_z = \frac{h^x_i h^y_j}{4}.$$

We will skip the details of approximation of the right-hand side of (3) and note only that we use the 3D analog of the quadrature trapezoidal formula for the volume integral.

After calculating all the entries of the local balance matrix and the local right-hand side vector in element-by-element traversing of all grid cells, the assembling procedure gives the global balance matrix and the global right-hand side vector of the final system of linear equations. One equation, say, for the grid node with the indices (i,j,k) has for u-component of the velocity vector the following form:

$$a^0_{i,j,k}u_{i,j,k} - a^1_{i,j,k}u_{i-1,j,k} - a^2_{i,j,k}u_{i,j-1,k} - a^3_{i,j,k}u_{i+1,j,k} - a^4_{i,j,k}u_{i,j+1,k} - a^5_{i,j,k}u_{i,j,k-1} - a^6_{i,j,k}u_{i,j,k+1} = g_{i,j,k}. \quad (4)$$

The global balance matrix is 3×3 block-diagonal matrix with the blocks having the same structure and even the same value of their entries in the case of the same boundary conditions for the velocity vector components. Each block is a seven-diagonal matrix. To save the storage space, the global matrix is represented in the form of a special row-wise sparse format [6].

So, the final system of nonlinear algebraic equations can be presented in the form

$$\overline{A}(\vec{u}) \cdot \vec{u} \equiv \begin{pmatrix} A^u(\vec{u}) & 0 & 0 \\ 0 & A^v(\vec{u}) & 0 \\ 0 & 0 & A^w(\vec{u}) \end{pmatrix} \begin{pmatrix} u \\ v \\ w \end{pmatrix} = \begin{pmatrix} g^u \\ g^v \\ g^w \end{pmatrix} = g. \quad (5)$$

A solution to this system is found by a low relaxation iterative process

$$\overline{A}(\vec{u}^m) \cdot \hat{u}^{m+1} = g, \quad u^{m+1} = \omega\hat{u}^{m+1} + (1-\omega)u^m, \quad m = 0,1,\ldots, \quad (6)$$

with a parameter $0 < \omega \leq 1$.

At each step of the nonlinear iteration (6), solution of the block linear non-symmetric system is found by a preconditioned biconjugate (multi-step) minimum residual method (BiMR). Because of non-symmetricity of the matrix, this algorithm does not posses a variational property, but it is the direct generalization of the MINRES method which has the global minimization of the functional (r^n, r^n) at each n-th iteration in the case of the symmetric positive definite system.

The preconditioning of the block matrix $\overline{A}$ in (6) is made by the explicit incomplete factorization technique $\tilde{A} = \overline{L}_B^{-1}\overline{A}\overline{U}_B^{-1}$, where $\overline{L}_B$ and $\overline{U}_B$ are the block-diagonal matrices with the blocks L_B, U_B defined in [6]. The iterations of the BiMR method are done according to the following formulas:

$$r^0 = g - \tilde{A}u^0, \quad \tilde{r}^0 = p^0 = \tilde{p}^0 = r^0,$$
$$\sigma_n = (\tilde{A}p^n, \tilde{A}^t p^n), \quad \rho_n = (\tilde{A}r^n, r^n), \quad \alpha_n = \frac{\rho_n}{\sigma_n},$$
$$u^{n+1} = u^n + \alpha_n p^n, \quad r^{n+1} = r^n - \alpha_n \tilde{A}p^n, \quad \tilde{r}^{n+1} = \tilde{r}^n - \alpha_n \tilde{A}^T \tilde{p}^n,$$
$$\beta_n = \frac{(\tilde{A}r^{n+1}, \tilde{r}^{n+1})}{(\tilde{A}r^n, r^n)}, \quad p^{n+1} = r^{n+1} + \beta_n p^n, \quad \tilde{p}^{n+1} = \tilde{r}^{n+1} + \beta_n \tilde{p}^n,$$

$$\tilde{A}p^{n+1} = \tilde{A}r^{n+1} + \beta_n \tilde{A}p^n, \quad \tilde{A}^t\tilde{p}^{n+1} = \tilde{A}^t\tilde{r}^{n+1} + \beta_n \tilde{A}^t\tilde{p}^n,$$
$$n = 0, 1, 2, \dots .$$

The stopping criterion for this process is the following:

$$\frac{(r^n, r^n)}{(g, g)} \leq \varepsilon^2 \ll 1.$$

Robustness of the BiMR method is provided by the multivariant restarts under the conditions

$$\alpha_{\min} < \alpha_n < \alpha_{\max}, \quad \beta_{\min} < \beta_n < \beta_{\max}.$$

The recommended values in these inequalities are $\alpha_{\min} = 0.01$, $\alpha_{\max} = 10$, $\beta_{\min} = 0$, $\beta_{\max} = 1$. In particular cases, these values should be chosen experimentally.

3. Numerical experiments

The aim of the experiments is to check the convergence of the algorithms and the truncation error if the exact analytical solution for the test is known.

In the tables below, we present the results of the numerical experiments. We give the values of the truncation errors

$$\delta_s = \max_{ijk} \|s(x_i, y_j, z_k) - s^h_{i,j,k}\|$$

on different grids and the numbers of iterations of the BiMR procedure. If the number of nonlinear velocity iterations is greater than 1, we present in the tables the final truncation errors and the numbers of iterations at every nonlinear phase of the solution process.

Also, we present the value of numerical divergence to look after its convergence to zero as the size of the grid steps decreases.

Test 1. The velocity field describes a flat current of the viscous incompressible fluid in a square cavity [7]. The exact solution is obtained by the following formulas:

$$u(x, z) = 8\zeta_1(x)\zeta_2'(z), \quad v(x, z) = 0, \quad w(x, z) = -8\zeta_1'(x)\zeta_2(z),$$
$$\zeta_1(x) = x^4 - 2x^3 + x^2, \quad \zeta_2(z) = -4z^4 + 10z^3 - 6z^2.$$

These velocities have the property $\operatorname{div} \vec{u} = 0$.

The vertical volume force ($f_y = f_x = 0$) and the pressure have the following analytical representations:

$$f_z = 8\Big(24\int \zeta_1(x) + 2\zeta_1'(x)\zeta_2''(z) + \zeta_1'''(x)\zeta_2(z)\Big) -$$
$$64\Big(\Big(\int \zeta_1(x)\zeta_1'(x)\Big)(\zeta_2(z)\zeta_2''''(z) - \zeta_2'(z)\zeta_2''(z)) -$$
$$\zeta_2(z)\zeta_2'(z)(\zeta_1(x)\zeta_1''(x) - \zeta_1'(x)\zeta_1'(x))\Big),$$
$$p(x,z) = 8\Big(24\Big(\int \zeta_1(x)\Big)\zeta_2''''(z) + 2\zeta_1'(x)\zeta_2'(z)\Big) +$$
$$64\Big(\int \zeta_1(x)\zeta_1'(x))(\zeta_2(z)\zeta_1''(z) - e2(z)\zeta_2(z)\Big).$$

The computational domain is a cube $\Omega = [0,1]^3$. The boundary conditions for the components are set as follows: $u = 0$ on $x = 0$, $x = 1$, $z = 0$ and $du/dn = 0$ on $y = 0$, $y = 1$, $z = 1$; $v = 0$ on all the cube faces; $w = 0$ on on $x = 0$, $x = 1$, $z = 0$, $z = 1$, $dw/dn = 0$ on $y = 0$, $y = 1$. The computational domain is discretized by the uniform grids with the step $h = 1/N$, $N = 8, 16, 32, 64$. The system of grid equations is iteratively solved by the BiMR method with the stopping criterion $\varepsilon = 10^{-10}$.

The number of the nonlinear velocity iterations equals 1. So, the velocity field components in this test are, on the one hand, coefficients in the equations of motion, but on the other hand, they are the sought for unknowns.

The initial guess for the iterative subroutine is the analytical solution, the initial velocity and pressure are also analytical. So, the aim of the test is to check the correctness of the approximation procedure and to present the convergence analysis when $h \to 0$.

The results of this test are shown in Table 1. Its last column has numbers of iterations of the BiMR procedure. Let us note that the truncation error for the velocity component v has order 10^{-16} which corresponds to zero value, so we omit these data in the table.

From this table one can see that as the truncation error decreases by the factor of four while the grid steps decrease by the factor of 2, the error is of order $O(h^2)$.

Moreover, the divergence tends to zero as the grid refines.

Table 1

N	δ_u	δ_w	δ_p	div $\vec{u}$	Num. of iter.
8	0.0264	0.0484	0.00381	0.476	17
16	0.00673	0.0126	0.00220	0.201	27
32	0.00170	0.00319	0.00118	0.0767	54
64	0.000429	0.000799	0.00110	0.0281	107

Test 2. This test is analogous to Test 1 but with zero initial guess for the iterative procedure and pressure and eight nonlinear velocity iterations.

The numerical results are almost the same as in Test 1 for the truncation errors, therefore we will give here only numbers of iterations of the BiMR procedure at each nonlinear iteration (Table 2).

Table 2

N	Number of iterations
8	21 – 21 – 17 – 16 – 11 – 8 – 0 – 0
16	37 – 37 – 29 – 23 – 19 – 14 – 0 – 0
32	64 – 64 – 59 – 48 – 40 – 0 – 0 – 0
64	126 – 126 – 115 – 100 – 83 – 0 – 0 – 0

It follows from the table data that eight nonlinear iterations provide their good convergence as the last iterations did not iterate at all (the number of iterations is zero).

Test 3. This test has the following analytical velocities with the property $\operatorname{div} \vec{u} = 0$ under any constant pressure:

$$
\begin{aligned}
u &= \sin^2 \pi x \sin \pi y \sin 2\pi z, \\
v &= \sin \pi x \sin^2 \pi y \sin 2\pi z, \\
w &= -(\sin 2\pi x \sin \pi y + \sin \pi x \sin 2\pi y) \sin^2 \pi z.
\end{aligned}
$$

The right-hand side functions f_u, f_v, f_w are analytically calculated from equations (1).

The computational domain is a cube $\Omega = [0,1]^3$. The boundary conditions for the velocity components are zero Dirichlet boundary conditions. The domain is discretized by a uniform grid with the step $h = 1/N$, $N = 8, 16, 32, 64$. A system of grid equations is iteratively solved by the BiMR method with the stopping criterion $\varepsilon = 10^{-10}$ (Table 3). The number of the nonlinear velocity iterations equals 1.

The initial guess for an iterative subroutine is the analytical solution, the initial velocities and pressure being analytical as well.

It follows from these data that the truncation error is also of order $O(h^2)$.

Table 3

N	$\delta_u = \delta_v$	δ_w	δ_p	$\operatorname{div} \vec{u}$	Num. of iter.
8	0.0946	0.125	0.0848	0.497	20
16	0.0235	0.0343	0.0494	0.207	31
32	0.00582	0.00869	0.0246	0.0764	51
64	0.00145	0.00219	0.0121	0.0272	77

References

[1] Chizhonkov E.V. On methods for solving the Stokes problem for a weakly-compressible and incompressible fluids // Advanced Mathematics: Computations and Applications. Proceedings of AMCA-95 / Eds.: A.S. Alekseev, N.S. Bakhvalov. – Novosibirsk, NCC Publisher. – 1995. – P. 167–171.

[2] Bramble J.H., Pasciak J.E., Vassilev A.T. Analysis of the inexact Uzawa algorithm for saddle point problems // SIAM J. Numer. Anal. – 1997. – Vol. 33, № 4. – P. 1072–1092.

[3] Kobel'kov G.M., Ol'shanskii M.A. Effective preconditioning of Uzawa type schemes for a generalized Stokes problem // Num. Math. – 2000. – Vol. 86. – P. 443–470.

[4] Gurieva Y.L., Il'in V.P. On the numerical solution of 3D diffusion-convection equations // Sib. J. Industrial Math. – 2003. – Vol. 6, № 1. – P. 27–34 (in Russian).

[5] Il'in V.P. On exponential finite volume approximations // RJNAMM. – 2003. – Vol. 18, № 6. – P. 479–506.

[6] Andreeva M.Y., Il'in V.P., Itskovich E.A. Two solvers for nonsymmetric SLAEs // *This issue.*

[7] Pereira J.M.C., Kobayashi M.H., et al. A fourth-order-accurate finite volume compact method for the incompressible Navier–Stokes solutions // J. Comp. Phys. – 2001. – Vol. 167. – P. 217–243.